

Numerical study of the two-dimensional Heisenberg model using a Green function Monte Carlo technique with a fixed number of walkers

Matteo Calandra Buonaura and Sandro Sorella

Istituto Nazionale di Fisica della Materia and International School for Advanced Study, Via Beirut 4, 34013 Trieste, Italy

(Received 4 November 1997; revised manuscript received 2 February 1998)

We describe in detail a simple and efficient Green function Monte Carlo technique for computing both the ground state energy and the ground state properties by the “forward walking” scheme. The simplicity of our reconfiguration process, used to maintain the walker population constant, allows us to control any source of systematic error in a rigorous and systematic way. We apply this method to the Heisenberg model and obtain accurate and reliable estimates of the ground state energy, the order parameter, and the static spin structure factor $S(q)$ for several momenta. For the latter quantity we also find very good agreement with available experimental data on the La_2CuO_4 antiferromagnet. [S0163-1829(98)04418-X]

I. INTRODUCTION

After almost one decade since the discovery of high- T_c superconductivity we have certainly understood much more about magnetism rather than superconductivity. In particular, since almost all the stoichiometric compounds of high- T_c superconductors are good antiferromagnets, well described by the two-dimensional Heisenberg model (HM), from the very beginning a strong numerical effort has been devoted to the simulation of this model.^{1,2} The HM is defined by the following Hamiltonian:

$$H_J = J \sum_{\langle i,j \rangle} \vec{S}_i \cdot \vec{S}_j, \quad (1)$$

where the spin one-half vectors \vec{S}_i satisfy $\vec{S}^2 = 3/4$ and J is the nearest-neighbor antiferromagnetic superexchange coupling, connecting nearest-neighbor pairs $\langle i,j \rangle$. Henceforth periodic boundary conditions are assumed in a finite square lattice with $N_a = l \times l$ sites.

Although a rigorous proof that this model has long-range antiferromagnetic order in two spatial dimensions is still lacking, there is a general consensus that long-range order exists even in this interesting case. In other words its properties should be very well understood by the simple spin-wave theory, which assumes long-range antiferromagnetic order in the ground state.³

In this work we give accurate ground state properties of the HM using a new and more efficient version of the Green function Monte Carlo (GFMC) technique, applied on a lattice by Trivedi and Ceperley, some years ago.²

With the present scheme we also estimate the ground state energy of the HM on the square lattice to be $-0.669\,442J \pm 0.000\,026J$ slightly different, but more accurate than the previous GFMC estimates. Analogously we obtain for the antiferromagnetic order parameter the value $m = 0.3077 \pm 0.0004$, consistent with other numerical estimates but with a very accurate control of the finite-size effects. We discuss also our results for the static spin structure factor in view of the recently proposed theory for the finite-size scaling in a quantum antiferromagnet.⁴ In particular we verify that, as a remarkable prediction of the theory, the small- q behavior of

this function behaves as $S(q) = \chi c|q|$, where χ is the magnetic spin susceptibility and c the spin-wave velocity of the HM. This relation is particularly important as this function is experimentally detectable in neutron scattering experiments.⁵

Let us discuss now the technical part of our work, which is based on the GFMC technique, as we have mentioned before. As is well known this technique allows one to sample statistically the ground state of a many-body Hamiltonian H by a set of walkers (w_i, x_i) which represent vectors wx of a large (or even infinite) Hilbert space. The set of all configurations x spans a normalized and complete basis. The aim of this approach is to sample statistically the ground state of H , by a large population of walkers.⁶ As it will be described later on, in the finite-dimensional case, the GFMC on a lattice is based on a statistical application of the Hamiltonian matrix-vector product $w'_i x'_i \rightarrow (-H) w_i x_i$ to the walker configurations $\{wx\}_i$, thus filtering out, after many iterations, the desired population distribution for the ground state. In this statistical iteration, however, the walker weights w_i increase or decrease exponentially so that after a few iterations most of the walkers have negligible weights and some kind of reconfiguration becomes necessary to avoid large statistical errors. The process to eliminate the irrelevant walkers or generate copies of the important ones is called “branching.” This scheme is in principle exact only if the population of walkers is let to increase or decrease without any limitation. Any reconfiguration of the population size may in fact introduce some spurious correlation between the walkers that may affect the statistical sampling of the ground state. In practice for a long simulation it is always necessary to control the population size, as, otherwise, one easily exceeds the maximum allowed computer memory. This control of the walker population size may introduce some kind of bias that vanishes quite slowly for an infinite number of walkers.^{6,7} In this case only by performing several runs with different numbers of walkers may one in principle estimate the size of the residual bias.

Following the Hetherington’s work,¹¹ we define here an efficient reconfiguration process at a fixed number M of walkers, with a rigorous control of the bias and without need of the conventional branching scheme.

In the last sections we present the results obtained for the HM up to an $N_a=16\times 16$ lattice size, together with some numerical tests on a small $N_a=4\times 4$ lattice where an accurate numerical solution is available by exact diagonalization. Previous calculations on this model, using the Green function Monte Carlo technique, were performed either without correcting the bias² and controlling it for small lattices with a large number of walkers or by correcting the bias in a way, which is probably correct, but is not possible to prove rigorously.⁸

II. GFMC TECHNIQUE

In the following sections we describe in detail how to evaluate the maximum eigenvector of a matrix $H_{x',x}$ with all positive definite matrix elements, using a stochastic approach. Clearly in any physical problem, described by a Hamiltonian H , the most interesting eigenvalue is the lowest one: the ground state energy. This is, however, just a matter of notation, as the ground state of H represents the maximum excited state of $-H$. In the following, for simplicity, we assume a change in the sign of H so that the physical ground state is, in this notation, the maximum eigenvector of H . More important instead is the restriction of positive definite matrix elements $H_{x',x}$, which drastically constrains the class of Hamiltonians that can be treated with this method, without facing the old but still unsolved “sign problem.” Whenever the Hamiltonian has matrix elements with arbitrary sign, schemes like the “fixed node approximation,” and their recent developments to finite lattices, are possible within the GFMC method.^{9,10} Of course, if negative signs occur only in the diagonal elements of H , a simple change of the Hamiltonian $H\rightarrow H_{x',x}+\lambda\delta_{x',x}$, will not change the ground state but the Hamiltonian will satisfy the condition $H_{x',x}\geq 0$ for a large enough shift λ . For instance, the Heisenberg Hamiltonian can be easily cast in the previous form as had been previously shown.²

From a general point of view the ground state of H can be obtained by applying the well-known power method:

$$|\psi_0\rangle=\lim_{L\rightarrow\infty}H^L|\psi_T\rangle, \quad (2)$$

where the equality holds up to (infinite) normalization, and $|\psi_T\rangle$ is a trial state nonorthogonal to the ground state $|\psi_0\rangle$.

In the following a simple stochastic approach is described for evaluating the state $H^M|\psi_T\rangle$. To this purpose we define a basic element of this stochastic approach: the so-called walker. A walker is determined by an index x corresponding to a given element $|x\rangle$ of the chosen basis and a weight w . The walker “walks” in the Hilbert space of the matrix H and assumes a configuration wx according to a given probability distribution $P(w,x)$.

The task of the Green function Monte Carlo approach is to define a Markov process, yielding after a large number n of iterations a probability distribution $P_n(w,x)$ for the walker which determines the ground state wave function ψ_0 . To be specific in the most simple formulation one has

$$\int dw w P(w,x)=\langle x|\psi_0\rangle.$$

III. SINGLE-WALKER FORMULATION

In the following the distribution $P(w,x)$ is sampled by a finite number M of walkers. Let us first consider the simpler case $M=1$. In order to define a statistical implementation of the matrix multiplication $|x\rangle\rightarrow H|x\rangle$, the standard approach is first to determine the Hamiltonian matrix elements $H_{i,x}$ connected to x which are different from zero. Then a new index x' is chosen for the walker among the indices i according to the probability determined by

$$p_{i,x}=H_{i,x}/b_x, \quad (3)$$

where $b_x=\sum_i H_{i,x}$ has been introduced in order to satisfy the normalization condition $\sum_i p_{i,x}=1$. This simple iteration scheme to go from a configuration x to a new configuration x' is easily implemented but is not sufficient to determine stochastically the matrix-vector product Hx . The full matrix is a product of a stochastic matrix $p_{i,x}$ and a diagonal one b_x :

$$H_{i,x}=p_{i,x}b_x. \quad (4)$$

As is intuitively clear the diagonal matrix b_x , not included in the stochastic process, is very easily determined by a scaling of the weight w of the walker:

$$w'\rightarrow b_x w. \quad (5)$$

The two previous updates, the stochastic one (3) and the deterministic one (5), define a new walker w',x' in place of the “old” walker w,x ; i.e., they determine a Markov process.

At this point it is important to understand the evolution of the probability distribution $P(w,x)$ after such process. A subscript n to this function P will indicate the number of iterations of the Markov process. The probability evolution $P_n\rightarrow P_{n+1}$ is easily determined by

$$P_{n+1}(w',x')=\sum_x p_{x',x}P_n(w'/b_x,x)/b_x. \quad (6)$$

Equation (6) allows us to determine, by simple iteration, what is the probability to find a walker in a given configuration w,x after many steps. However the evolution P_n from the initial distribution P_0 is more clear and transparent in terms of its momenta over the weight variable w :

$$G_{k,n}(x)=\int dw w^k P_n(w,x). \quad (7)$$

In fact it is straightforward to verify, using Eq. (6), that

$$G_{k,n+1}(x')=\sum_x p_{x',x}b_x^k G_{k,n}(x). \quad (8)$$

In particular for $k=1$ the first momentum of P determines the full quantum mechanical information, as $G_{1,n}(x')=(H^n)_{x',x}G_{1,0}(x)$, implying that $G_{1,n}(x)$, by Eq. (2), converges to the ground state of the Hamiltonian H .

By iterating several times even a single walker, the resulting configuration w,x will be distributed according to the

ground state of H and by sampling a large number of independent configurations we can evaluate, for instance, the ground state energy:

$$E_0 = \frac{\langle wb_x \rangle}{\langle w \rangle}, \quad (9)$$

where the brackets $\langle \rangle$ indicate the usual stochastic average, namely, averaging over the independent configurations.

This in principle concludes the GFMC scheme. However, the weight w of the walker grows exponentially with n (simply as a result of n independent products) and can assume very large values, implying a diverging variance in the above averages.

In the next sections we describe in detail this problem and a way to solve it with a *fixed* number of walkers.

IV. STATISTICAL AVERAGE DURING THE MARKOV PROCESS

The configurations x_n that are generated in the Markov process are distributed after a long time according to the maximum right eigenstate $R(x)$ of the matrix $p_{x',x}$ [simply because $G_{n,0}(x) = \sum_{x'} (p^n)_{x,x'} G_{0,0}(x') \rightarrow R(x)$ for large n] which, as we have seen, is in general different from the ground state $\psi_0(x)$ we are interested in, due to the weights w_n that weight differently the various configurations x distributed according to $R(x)$. We are allowed to consider this state $R(x)$ as the initial trial state $|\psi_T\rangle$ used in the power method (2), and that, at any Markov iteration n , the walker had weight $w=1 \dots L$ iterations backward, when it was at equilibrium according to the distribution $R(x)$, described before. In this way it is simple to compute the global weight of the walker with L power method correcting factors:

$$G_n^L = \prod_{j=1}^L b_{x_{n-j}}. \quad (10)$$

Therefore, for instance, in order to compute the energy with a single Markov chain of many iterations, the following quantity is usually sampled:

$$E_0 = \frac{\sum_n b_{x_n} G_n^L}{\sum_n G_n^L}, \quad (11)$$

with L fixed.¹¹ The reason for taking L as small as possible is that for large L the weight factors G_n^L diverge exponentially, leading to uncontrolled fluctuations. In order to compute the variance of the G_n^L factors we can simply apply what we have derived in the previous section and prove in a few lines the exponential growth of the fluctuations of the weights. Using Eq. (7) it is easily found that

$$(\delta G^L)^2 = G_{2,L}(x) - G_{1,L}(x)^2.$$

According to Eq. (8) $G_{2,L}$ for large L diverges exponentially fast as λ_2^L where λ_2 is the maximum eigenvalue of the matrix pb^2 (b is here a diagonal matrix $b = \delta_{x,x'} b_x$), whereas the first momentum $G_{1,L}$ diverges as $G_{1,L} \sim \lambda^L$, with λ the maxi-

mum eigenvalue of the Hamiltonian matrix $H=pb$. It is clear therefore that we get an exponential increase of the fluctuations,

$$(\delta G^L)^2 \sim (\lambda_2^L - \lambda^{2L}),$$

as in general $\lambda_2 > \lambda^2$ and the equality sign holds only if the matrix b is a constant times the identity matrix.

In order to overcome the problem of an exponentially increasing variance, in the following section we will discuss a way to propagate a set of M walkers simultaneously. By evolving them independently, clearly no improvement is obtained for the aforementioned large fluctuations, as for this purpose it is equivalent to iterating longer a single walker. Instead, before the variance of the weights w_i becomes too large, it is better to redefine the set of walkers by dropping out the ones with a weight which is too small, and correspondingly generate copies of the more important ones, so that after this reconfiguration all the walkers have approximately the same weight. By iterating this process the weights of all the walkers are kept approximately equal during the simulation. This property yields a considerable reduction of the statistical errors, as the variance of the average weight $\bar{w} = (1/M) \sum_i w_i$ is reduced by a factor of \sqrt{M} . This allows therefore a more stable propagation even for large L .

V. CARRYING MANY CONFIGURATIONS SIMULTANEOUSLY

Given M walkers we indicate the corresponding configurations and weights with a couple of vectors $(\underline{w}, \underline{x})$, with each vector component $w_i, x_i, i = 1, \dots, M$, corresponding to the i th walker. It is then easy to generalize Eq. (6) to many independent walkers:

$$\begin{aligned} P_{n+1}(\underline{w}, \underline{x}) = & \sum_{x'_1, x'_2, \dots, x'_M} P_n(w_1/b_{x_1}, w_2/b_{x_2}, \dots, w_M/b_{x_M}, \\ & b_{x'_M}, x'_1, x'_2, \dots, x'_M) \\ & \times (p_{x_1, x'_1} p_{x_2, x'_2} \cdots p_{x_M, x'_M}) / (b_{x_1} b_{x_2} \cdots b_{x_M}). \end{aligned} \quad (12)$$

If the evolution of P is done without further restriction, each walker is uncorrelated from any other one and

$$\begin{aligned} P(w_1, w_2, \dots, w_M, x_1, x_2, \dots, x_M) \\ = P(w_1, x_1) P(w_2, x_2) \cdots P(w_M, x_M). \end{aligned}$$

Similarly to the previous case we can define the momenta over the weight variable:

$$\begin{aligned} G_{k,n}(x) = & \int dw_1 \int dw_2 \cdots \int dw_M \sum_x \\ & \times \left(\frac{w_1^k \delta_{x,x_1} + w_2^k \delta_{x,x_2} + \cdots + w_M^k \delta_{x,x_M}}{M} \right) P_n(\underline{w}, \underline{x}). \end{aligned} \quad (13)$$

Since we are interested only in the first momentum of P , we can define a reconfiguration process that changes the

probability distribution P_n without changing its first momentum, and in this we follow Ref. 11:

$$P'_n(\underline{w}', \underline{x}') = \int \sum_{\underline{x}} G(\underline{w}', \underline{x}'; \underline{w}, \underline{x}) P(\underline{w}, \underline{x}) [d\underline{w}], \quad (14)$$

$$G(\underline{w}', \underline{x}'; \underline{w}, \underline{x}) = \prod_{i=1}^M \left(\frac{\sum_j w_j \delta_{x_i', x_j}}{\sum_j w_j} \right) \delta\left(w_i' - \frac{\sum_j w_j}{M}\right). \quad (15)$$

Hereafter the multiple integrals over all the w_j variables are expressed conventionally in shorthand by $\int [d\underline{w}]$. Note that the defined Green function G is normalized, $\int [d\underline{w}'] \sum_{\underline{x}'} G = 1$.

In practice this reconfiguration process amounts to generate a new set of M walkers (w'_j, x'_j) in terms of the given M walkers (w_j, x_j) in the following way. Each new walker w'_j, x'_j will have the same weight $\bar{w} = \sum_j w_j / M$ and an arbitrary configuration x'_j among the possible old ones x_k , $k = 1, \dots, M$, chosen with a probability $p_k = w_k / \sum_j w_j$. It is clear that after this reconfiguration the new M walkers have by definition the same weights and most of the irrelevant walkers with small weights are dropped out. This is just the desired reconfiguration which plays the same stabilization effect of the conventional branching scheme.² For an efficient implementation of this reconfiguration scheme see the Appendix.

VI. BIAS CONTROL

It is well known that control of the population size M introduces some bias in the simulation simply because some kind of correlation between the walkers is introduced. However, for high-accuracy calculations this bias often becomes the most difficult part to control. In this section we can instead prove that the reconfiguration of the M walkers defined in Eq. (14) does a better job. Though this reconfiguration clearly introduces some kind of correlation among the walkers, it can be rigorously proved that the first momentum $G_{1,n}(x)$ of the distribution of P is exactly equal to the one $G'_{1,n}(x)$ of P' , obtained after reconfiguration. This means that there is no loss of information in the described reconfiguration process and

$$G'_{1,n}(x) = G_{1,n}(x). \quad (16)$$

Proof. By definition using Eqs. (13) and (14),

$$\begin{aligned} G'_{1,n}(x) &= \int [d\underline{w}] \int [d\underline{w}'] \sum_{\underline{x}, \underline{x}'} \left(\frac{\sum_j w'_j \delta_{x, x'_j}}{M} \right) \\ &\quad \times G(\underline{w}', \underline{x}'; \underline{w}, \underline{x}) P(\underline{w}, \underline{x}). \end{aligned}$$

The first term in the integrand contains a sum. It is simpler to single out each term of the sum $w'_k \delta_{x, x'_k} / M$ and to integrate over all the possible variables $\underline{w}', \underline{x}'$ but w'_k and x'_k . It is then easily obtained that this contribution to $G'_{1,n}$ conventionally indicated as $[G'_{1,n}]_k$ is given by

$$\begin{aligned} [G'_{1,n}]_k &= \int [d\underline{w}] \int [d\underline{w}'] \sum_{\underline{x}, \underline{x}'_k} \frac{w'_k}{M} \delta_{x, x'_k} \left(\frac{\sum_j w_j \delta_{x'_k, x_j}}{\sum_j w_j} \right) \\ &\quad \times \delta\left(w'_k - \frac{\sum_j w_j}{M}\right) P(\underline{w}, \underline{x}). \end{aligned}$$

Then by integrating simply in $d\underline{w}'$ and summing over x'_k in the previous integrand we easily get that $[G'_{1,n}]_k = (1/M) G_{1,n}$, independent of k . Finally by summing over k we prove the statement (16).

VII. GFMC SCHEME WITH BIAS CONTROL

Using the previous result it is easy to generalize Eqs. (10) and (11) to many configurations. It is assumed that the reconfiguration process described in the previous section is applied iteratively each k_b step of independent walker propagation. The index n appearing in the old expressions (10) and (11) now labels the n th reconfiguration process. The measurement of the energy can be done after the reconfiguration when all the walkers have the same weight; thus, in Eq. (10),

$$b_{x_n} \rightarrow b_{\underline{x}_n} \rightarrow \frac{1}{M} \sum_{j=1}^M b_{x_j^n} \quad (17)$$

or, for a better statistical error, the energy can be sampled just before the reconfiguration, taking properly into account the weight of each single walker:

$$b_{\underline{x}_n} = \frac{\sum_{j=1}^M w_j b_{x_j^n}}{\sum_{j=1}^M w_j}. \quad (18)$$

It is important, after each reconfiguration, to save the quantity $\bar{w} = (1/M) \sum_{j=1}^M w_j$ and reset to 1 the weights of each walker. Thus the total weights G_n^L correspond to the application of $L k_b$ power method iterations [as in Eq. (2)] to the equilibrium distribution $\psi_T(x) = G_{0,n-L}(x)$, which at equilibrium is independent of n . The value of the factor G_n^L can be easily recovered by following the evolution of the M walkers in the previous L reconfiguration processes and reads

$$G_n^L = \prod_{j=0}^{L-1} \bar{w}_{n-j}, \quad (19)$$

where the average weight of the walkers \bar{w} has been defined previously.

An example of how the method works for the calculation of the ground state energy of the HM in a 4×4 lattice is shown in Fig. 1. Remarkably our method converges very fast to the exact result with few correcting factors and with smaller error bars as compared with the original Hetherington scheme. Our method does not require the population control reconfiguration at each step, and the resulting bias is considerably reduced, in the sense that, without any correcting factor, our value is 5 times closer to the exact result, for the example shown in Fig. 1.

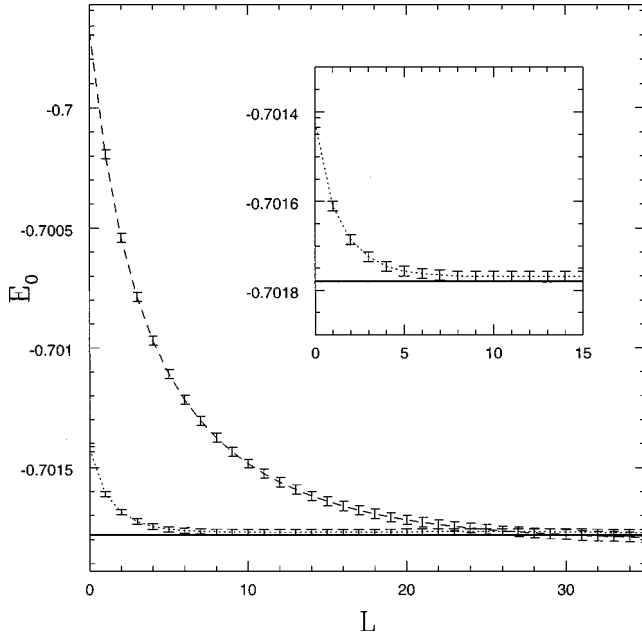


FIG. 1. Energy per site in a 4×4 Heisenberg cluster. The solid line is the exact result and the dotted (dashed) line connects GFMC data as a function of the number L of correcting factors within our scheme (Hetherington's one) described at the end of the Appendix. The number of walkers in this case was $M=10$ and the reconfiguration scheme was applied to each of four ($k_p=4$ in the text) iterations, while in the Hetherington's scheme $k_p=1$. The guiding wave function is given in Eq. (21) with $\gamma=1.2$, and all the data are obtained with the same amount of computer time. The inset is an expansion of the bottom-left part of the picture.

VIII. IMPORTANCE SAMPLING

One of the most important advantages of the Green function Monte Carlo technique is the possibility to reduce the variance of the energy by exploiting some information on the ground state wave function, sometimes known *a priori* on physical grounds. In order to understand how to reduce this variance, we just note that the method, as described in the previous sections, is not restricted to symmetric matrices, simply because we never used this property of the Hamiltonian matrices. Following Ref. 7 we consider not the original matrix, but the nonsymmetric one

$$H'_{x',x} = \psi_G(x') H_{x',x} / \psi_G(x),$$

where ψ_G is the so-called *guiding wave function*, which has to be as simple as possible to be efficiently implemented in the calculation of the matrix elements and, as we will see, as close as possible to the ground state of H .

In order to evaluate the maximum eigenvalue of H' , corresponding obviously to the ground state of H , the coefficient b_x is now given by H' as indicated in Eq. (11); in this case b_x reads

$$b_{x_n} = \sum_{x'} \psi_G(x') H_{x',x_n} / \psi_G(x_n). \quad (20)$$

Thus, if ψ_G is exactly equal to the ground state of H , then, by definition, $b_{x_n} = E_0$, independent of x_n . This is the so-called *zero variance property* satisfied by the method.

Namely, if the guiding wave function approaches an exact eigenstate of H , the method is free of statistical fluctuations. Of course one is never in such a fortunate situation, but by improving the guiding wave function one is able to considerably decrease the error bars of the energy. This property, rather obviously, is very important and nontrivial.

For the application of the method to the HM we have used a Jastrow-like guiding function

$$|\psi_G\rangle = \sum_x s_M(x) \exp\left(\frac{\gamma}{2} \sum_{R,R'} v(R-R') S_R^z S_{R'}^z\right) |x\rangle, \quad (21)$$

where $|x\rangle$ indicates in this case all possible spin configurations with $S_R^z = \pm \frac{1}{2}$ defined on each site R of the $l \times l$ square lattice and with the restriction of total vanishing spin projection $\sum_R S_R^z = 0$; $s_M(x)$ represents the so-called Marshall sign, depending on the number $N_\uparrow(x)$ of spin up in one of the two sublattices $s_M(x) = (-1)^{N_\uparrow(x)}$, while the long-range potential is given by

$$v(R) = \frac{2}{l^2} \sum_{q \neq 0} e^{iqR} \left[1 - \sqrt{\frac{1 + (\cos q_x + \cos q_y)/2}{1 - (\cos q_x + \cos q_y)/2}} \right],$$

with $|q_x| \leq \pi$ and $|q_y| \leq \pi$ belonging to the Brillouin zone and assuming the appropriate discrete values of a finite system with periodic boundary conditions. The constant γ is the only variational parameter in the wave function, which for $\gamma=1/2S$ is consistent with the spin-wave theory solution of the HM for large spin S .¹²

IX. FORWARD WALKING

The Green function Monte Carlo technique can be used with success to compute also correlation functions on the ground state of H . In fact it is simple to compute expectation values of operators that are diagonal in the chosen basis, so that to a given element x of the basis corresponds a well-defined value $O(x) = \langle x | O | x \rangle$ of the operator. By the Green function Monte Carlo technique, as we have seen, configurations w, x distributed according to the desired wave function $\psi_0(x)$, or $\psi_0(x)\psi_G(x)$ if importance sampling is implemented, are generated stochastically. However in order to compute $\langle O \rangle = \langle \psi_0 | O | \psi_0 \rangle$ a little further work is necessary as the square of the wave function is required to perform the quantum average. To this purpose the desired expectation value is written in the following form:

$$\langle O \rangle = \lim_{N', N \rightarrow \infty} \frac{\langle \psi_G | H^{N k_h} O H^{N' k_h} | \psi_G \rangle}{\langle \psi_G | H^{(N'+N)k_h} | \psi_G \rangle}. \quad (22)$$

From the statistical point of view Eq. (22) amounts first to sample a configuration x after N' GFMC reconfigurations, then to measure the quantity $\langle x | O | x \rangle$, and finally to let the walker propagate forward for further N reconfigurations.

In order to evaluate the stochastic average an approach similar to that done for the energy is clearly possible. The only change to expression (11) is to replace b_{x_j} with the average measured quantity $O_{\bar{x}_N} = (1/M) \sum_j O_j^n$ at the generation n and change the corresponding weight factors in Eq. (19) as

$$G_n^L = \prod_{j=-N}^{L-1} \overline{w}_{n-j}, \quad (23)$$

where henceforth we denote with O_j^n the value of the diagonal operator O on the configuration x_j of the j th walker, at the iteration n . Indeed these new factors (23) contain a further propagation of N reconfiguration processes as compared to the previous expression. It is important that both L , correcting the bias, and N , correcting the quantum average of the operator, are finite, due to the exponential growths of the fluctuations as N and L increase. On the other hand, these fluctuations can be controlled by enlarging the population size M , and the method for M large enough remains stable.

A further condition is, however, necessary in order to control the bias in the forward walking technique. The set of measured values O_i^n with weight factors (23) has to be modified after each reconfiguration process occurring in the forward direction. In practice after each reconfiguration it is important to bookkeep only the values O_i of the observables that survive after the reconfiguration (we omit in the following the superscript n for simplicity). In other words, after each reconfiguration $O'_i = O_{j(i)}$ for $i=1, \dots, M$ with the integer function $j(i)$ describing the reconfiguration process in our scheme [after any reconfiguration the walker with index i assumes the configuration with index $j(i)$ before the reconfiguration].

In order to implement recursively the forward walking it is useful to store at each reconfiguration process the integer function $j_n(i)$ for each reconfiguration n and the values O_i of the operator O for each walker. Then it is possible to compute the relevant configurations contributing to the operator O after N reconfiguration processes by a recursive application of the integer functions j_n , namely, $O'_i = O_{j_N[j_{N-1} \dots j_1(i) \dots]}$.

It is extremely important to perform the reconfiguration process as rarely as possible since after each reconfiguration in the forward direction the number of different configurations representing an operator O decays quickly, yielding of course a larger variance. Contrary to the Hetherington¹¹ algorithm our scheme allows bias control without requiring the reconfiguration at each step.

An example on how this scheme works is shown in Fig. 2. As is seen it is simple to reach the exact ground state average.

X. FORMAL PROOF OF THE BIAS CONTROL IN THE FORWARD WALKING SCHEME

In order to implement stochastically Eq. (22) we need to apply the operator O_x diagonal in configuration space, in a stochastic sense, and then follow the standard stochastic iteration (6) to the walker distribution P for N steps. To this purpose a walker from now on is identified by the triad

$$w, \gamma, x,$$

where γ represents the actual value of the measured operator O for the walker. Its value can change, as we will see later on in the reconfiguration process, and in general due to the forward walking $\gamma \neq \langle x | O | x \rangle$. Indeed only at the beginning, $n=0$, of the forward walking iteration $\gamma_i = O_i = \langle x_i | O | x_i \rangle$,

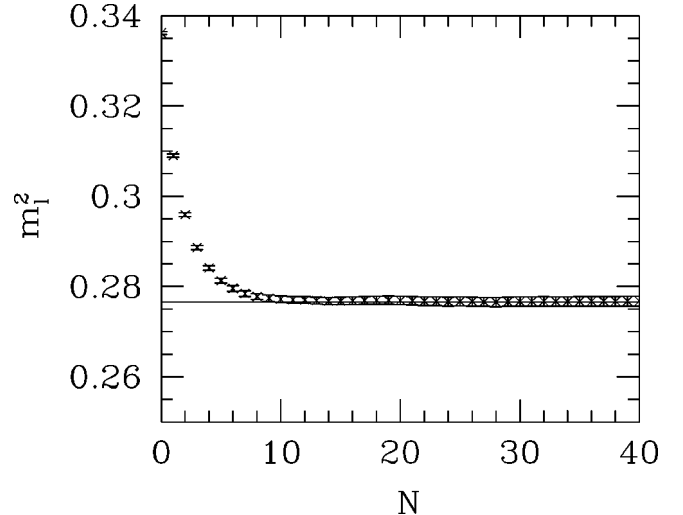


FIG. 2. Plot of the squared antiferromagnetic order parameter m_l^2 , in a 4×4 Heisenberg cluster as a function of the number N of forward walking reconfigurations. The solid line indicates the exact result. The number of walkers was fixed to $M=20$ with $k_p=5$. The guiding function was the one referenced in Fig. 1. With the present technique the z component of m_l can be measured on each sampled configuration; $m_l^z = (1/N_a) \sum_R (-1)^R S_R^z$ and spin isotropy is used to determine $m_l^2 = 3 \langle (m_l^z)^2 \rangle$.

for $i=1, \dots, M$. In a probabilistic sense this is equivalent to considering the initial probability distribution

$$P_{n=0}(w, \gamma, x) = P_0(w, x) \prod_{i=1, M} \delta(\gamma_i - O_i),$$

where P_0 is the equilibrium distribution of the previous Markov process (6), which samples the ground state $\psi_0(x)$.

With this initial condition further N forward walking steps are implemented to the probability distribution P , defined with the iterations in Eq. (6) and in Eq. (12). Then in order to determine the quantity (22) the following ratio is evaluated:

$$\langle O \rangle = \frac{\langle w \gamma \rangle}{\langle w \rangle}, \quad (24)$$

where the brackets indicate the average over the distribution $\sum_x dw \int d\gamma P(w, \gamma, x)$. It is understood that in Eq. (6) and Eq. (12) the variables γ_i remain unchanged. For instance the analogy of Eq. (6) will be

$$P_{n+1}(w', \gamma', x') = \sum_x p_{x', x} P_n(w'/b_x, \gamma', x)/b_x. \quad (25)$$

However, in order to satisfy the bias control property described in Sec. VI it is necessary to update the γ variables at any reconfiguration process.

Analogously to the previous case it is easier to work with $w \gamma$ momenta of order k of the distribution P for fixed configuration x [see Eq. (7)]:

$$G_{k,n}^\gamma(x) = \int dw \int d\gamma (w \gamma)^k P_n(w, \gamma, x), \quad (26)$$

which for $M=1$ corresponds to

$$G_{k,n}^{\gamma}(\underline{x}) = \int d\underline{w} \int d\underline{\gamma} \sum_{\underline{x}} \left(\frac{\sum_j (w_j \gamma_j)^k \delta_{x,x_j}}{M} \right) P_n(\underline{w}, \underline{\gamma}, \underline{x}), \quad (27)$$

where, as usual, underlined variables represent vectors whose components refer to the single-walker index j .

With a proof exactly analogous to the one of Sec. VI it is possible to show the following.

(i) The value of the first $(w\gamma)$ momentum $G_{1,n}^{\gamma}(\underline{x})$, at the initial iteration of the forward walking $n=0$, is equivalent to applying the operator O to the initial distribution $P_0(w, \underline{x})$, namely,

$$G_{1,n=0}^{\gamma}(\underline{x}) = O_x G_{1,n=0}(\underline{x}).$$

(ii) The following reconfiguration process, which does not change the Markov chain of configurations $(\underline{w}, \underline{x})$ but modifies slightly $\underline{\gamma}$, has the bias control property also for the $w\gamma$ averages:

$$P'_n(\underline{w}', \underline{\gamma}', \underline{x}') = \int \int \sum_{\underline{x}} G(\underline{w}', \underline{\gamma}', \underline{x}'; \underline{w}, \underline{\gamma}, \underline{x}) P(\underline{w}, \underline{\gamma}, \underline{x}) \times [d\underline{w}] [d\underline{\gamma}],$$

$$G(\underline{w}', \underline{\gamma}', \underline{x}'; \underline{w}, \underline{\gamma}, \underline{x}) = \prod_{i=1}^M \delta \left(\gamma'_i - \frac{\sum_j w_j \gamma_j \delta_{x'_i, x_j}}{\sum_j w_j \delta_{x'_i, x_j}} \right) \times \left(\frac{\sum_j w_j \delta_{x'_i, x_j}}{\sum_j w_j} \right) \delta \left(w'_i - \frac{\sum_j w_j}{M} \right). \quad (28)$$

The first factors in the Green function G , involving the γ 's, represent the only difference to the previous reconfiguration process (14). Thus obviously the momenta $G_{k,n}$ not involving the γ variables satisfy the same bias control property of the previous reconfiguration process (14).

As far as the $(w\gamma)$ momenta are concerned, it is possible to prove as before the mentioned bias control property

$$G'_{1,n}^{\gamma}(\underline{x}) = G_{1,n}^{\gamma}(\underline{x}). \quad (29)$$

To this purpose, analogously to the previous case, it is convenient to single out a term $j=k$ in the definition of the first $w\gamma$ momentum in Eq. (27), and following the same route of Sec. VI integrate easily the Green function over all possible variables w' , γ' , and x' , but the variables x'_k , γ'_k , and w'_k . These remaining integrations can be also performed analytically by first integrating in w_k , then in γ_k , and finally summing over x_k . The assertion (29) is therefore proved rigorously.

XI. "STRAIGHT"-FORWARD WALKING

A simpler method to compute averages of general operators is obtained by Eq. (24), performing two independent simulations for the numerator and the denominator in Eq. (24). The remarkable advantage of this technique is the possibility to measure also off-diagonal operators $O_{x',x}$. After

the first simulation for the evaluation of the denominator we take an equilibrated walker configuration (w, \underline{x}) and apply the operator O . Whenever the operator O is off diagonal this is not simply equivalent to scale the weight $w \rightarrow w O_x$. In fact we need a stochastic approach to select only one of the configurations x' among the possible ones connected to x with nonzero matrix element $O_{x',x}$. Whenever $O_{x',x} > 0$ this stochastic approach can be implemented with a two-step technique analogous to the one for the Hamiltonian as follows.

(i) We first scale w by the mixed average estimate $\sum_{x'} \psi_G(x') O_{x',x} / \psi_G(x)$.

(ii) Then we select a random new configuration x' with a probability proportional to $\psi_G(x') O_{x',x} / \psi_G(x)$.

Then the same reconfiguration process (14) to work with a fixed number of walkers during the forward walking propagation can be efficiently applied.

Finally we comment that the general operators O with arbitrary signs in the matrix elements can be always cast as a difference $O = O^+ - O^-$ of two operators with positive definite matrix elements; the above method can be applied to O^+ and O^- separately.

XII. DISCUSSION AND RESULTS

In the previous sections we have described how to obtain ground state energies and correlation functions of some class of Hamiltonians on a finite lattice size. In this section we describe a successful application of this method to the HM.

We are interested in thermodynamically converged physical quantities characterizing the quantum antiferromagnet, for instance, the energy per site e_0 , the staggered magnetization m , the spin-wave velocity c , and the spin susceptibility χ . Use of a finite-size scaling analysis is required to obtain the infinite-volume limit of our data.

We compute with our method the ground state energy per site, e_0 , and the ground state expectation value of the spin-spin structure factor $S(q)$:

$$S(q) = \frac{1}{N_a} \left\langle \psi_0 | \sum_{R,R'} e^{iq(R-R')} S_R \cdot S_{R'} | \psi_0 \right\rangle, \quad (30)$$

which for q equal to the antiferromagnetic momentum $Q = (\pi, \pi)$ allows a finite size estimate of the order parameter $m_l = \sqrt{S(Q)/N_a}$. The known finite-size scaling theory^{13,4} in a quantum antiferromagnet predicts that (a) the ground state energy per site, e_0 , has the following leading size corrections:

$$e_0(L) = e_0 - 1.4372c/l^3 + \dots, \quad (31)$$

which allows an indirect evaluation of the spin-wave velocity. (b) Further the finite-size estimate of the order parameter m_l approaches its converged value as $1/l$.

Finally Neuberger and Ziman,⁴ using a relativistic pion physics analogy, derived very powerful constraints on the spin-spin structure factor $S(q)$, namely, that for $q \rightarrow Q$ it diverges as $1/|q - Q|$ with a prefactor equal to $m^2/\chi c$. Using their arguments it also follows immediately that

$$S(q) \sim \chi c |q| \quad (32)$$

for $|q| \rightarrow 0$.

TABLE I. Energy per site of the HM in the square lattice $l \times l$. In this work the infinite-size extrapolation is obtained with a parabolic fit $E_0(l) = E_0(\infty) + a/l^3 + b/l^4$ for all size with $l \geq 8$. ($a = -2.275 \pm 0.12$ and $b = 1.64 \pm 0.9$). The numbers in parentheses represent error bars in the last digits.

l	E_0^{a}	E_0^{b}	E_0^{c}
6	-0.678871(8)	-0.678873(4)	-0.6788721(28)
8	-0.673486(14)	-0.673487(4)	-0.673483(8)
10	-0.671492(27)	-0.671549(4)	-0.671554(6)
12	-0.670581(49)	-0.670685(5)	-0.670678(5)
14	=	-0.670222(7)	-0.670223(8)
16	-0.669872(28)	-0.669976(7)	-0.669977(8)
∞	-0.66934(3)	-0.669437(5)	-0.669442(26)

^aReference 8.

^bReference 14.

^cThis work.

In spin-wave theory results for the constants appearing in Eq. (31) are given by

$$m = s - c', \quad (33)$$

$$c = 2Js\sqrt{2}(1 + c_0/2s), \quad (34)$$

$$\chi c = \frac{s}{2\sqrt{2}}(1 - c'/s), \quad (35)$$

where c_0 and c' can be estimated on a $l \times l$ finite size lattice,

$$c_0(l) = 1 - \frac{1}{N_a} \sum_k \epsilon_k \rightarrow 0.1579 \quad (36)$$

and

$$c'(l) = \frac{1}{2N_a} \sum_{k \neq 0, Q} \frac{1}{\epsilon_k} - \frac{1}{2} \rightarrow 0.1966, \quad (37)$$

and are expressed in terms of the spin-wave energy $\epsilon_k = \sqrt{1 - \gamma_k^2}$, where $\gamma_k = (\cos k_x + \cos k_y)/2$.

In order to improve the accuracy of the finite-size scaling calculation we have systematically compared our finite-size data with the spin-wave expansion on the same lattice sizes.¹⁵ This technique allows us to compute explicitly the finite-size corrections using the 1/S expansion, yielding results consistent with the previous theory for the finite-size corrections. The advantage of using finite-size spin-wave theory is that it also implicitly determines all the subleading corrections in $1/l$. In this approach, the energy per site is given by

$$e(l) = -2J \left[\frac{[s - c_0(l)]^2 - 1}{N_a^2} \right], \quad (38)$$

which correctly reproduces the predicted finite-size scaling (31) with the spin-wave velocity given by Eq. (35) and a finite-size next leading contribution $+2J/l^4$, appearing in the second-order spin-wave expansion. The latter term is inconsistent with a claim by Fisher, which probably omitted higher-order contributions in his analysis.¹³ On the other hand, the fit of the data reported in Table I is also in quan-

titative agreement with spin-wave theory, also for this next leading contribution to the energy per site.

By a simple Fourier transform of the finite-size spin-wave results for $\langle \vec{S}_R \cdot \vec{S}_0 \rangle$ we obtain $S(q) = 0$ for $q = 0$, consistent with a singlet ground state and

$$S(Q) = N_a [s - c'(l)]^2 - 1/N_a + \frac{1}{2N_a} \sum_{k \neq 0, Q} \left(\frac{\gamma_k}{\epsilon_k} \right)^2, \quad (39)$$

$$S(q) = \frac{1 - \gamma_q}{\epsilon_q} [s - c'(l)] - \frac{1}{N_a} + \frac{1}{4N_a} \times \sum_{k \neq 0, Q, q, q+Q} \frac{1 - \gamma_k \gamma_{q-k} - \epsilon_k \epsilon_{q-k}}{\epsilon_k \epsilon_{q-k}}, \quad q \neq Q, 0. \quad (40)$$

After a simple inspection the leading behavior $S(q) \propto |q|(S(q) \propto 1/|q - Q|)$ for $q \rightarrow 0$ ($q \rightarrow Q$) is in agreement with the Neuberger-Ziman predictions, with an exactly consistent prefactor $\chi c = (s/2\sqrt{2})(1 - c'/s)[m^2/\chi c = 2\sqrt{2}s(1 - c'/s)]$ within 1/s expansion.

Now we discuss the finite-size results obtained with the GFMC technique described in this paper.

First we compute the ground state energy per site e_0 and report all the data in Table I. According to Eq. (31) we make a parabolic fit in $1/l$ and obtain for the energy per site in the thermodynamic limit the value reported in Table I. This value differs from a previous GFMC estimate,⁸ without a population control error, which is exactly removed in our method. This error seems to affect significantly the large size estimate of the energy as shown in the Table I. A recent paper by Sandvik,¹⁴ using a completely different path integral method, reports energy values perfectly consistent with ours and with similar error bars. The spin-wave velocity is then evaluated by looking at the finite-size corrections of e_0 . Then according to Eq. (31) we obtain

$$c/c_{\text{SW}} = 1.12 \pm 0.06, \quad (41)$$

with $c_{\text{SW}} = \sqrt{2}J$ the zero-order spin-wave velocity. We have reached a very poor accuracy for this quantity, as it is determined by the subleading corrections of the energy, which in turn are also quite size dependent. For this quantity it is not possible to find significant differences from the second-order spin-wave result $c/c_{\text{SW}} = 1.1579$ [Eq. (35)], which is probably a more realistic and accurate value.

The order parameter is evaluated by the forward walking technique with (Sec. IX) or without (Sec. XI) bookkeeping of the branching matrix. In the latter case the spin isotropic square order parameter $S(Q)/N_a$ is directly evaluated, as the method is not restricted to diagonal operators. As discussed in this paper the only source of systematic errors is given by the length of the forward walking propagation N and the number of bias-correcting factors L for the ground state. It is understood that for $N, L \rightarrow \infty$ our method provides the exact finite-size value for m_l . The finite L error is negligible, as we have used a large enough number of walkers to eliminate the bias with few correcting factors.

The most important systematic error is due to the finite N . Its drastic and controlled reduction as a function of N is displayed in Fig. 3 which shows that we have achieved con-

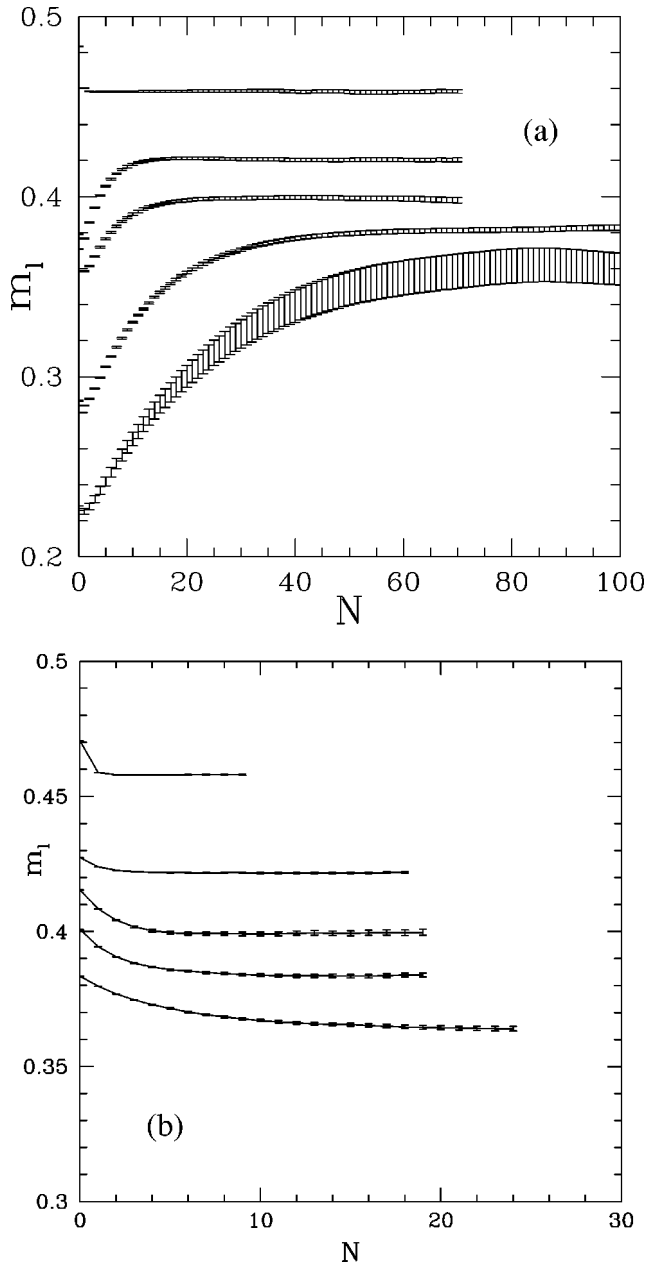


FIG. 3. Staggered magnetization for increasing lattice sizes (from top curve to bottom curve) as a function of the forward walking iteration number N computed with the method of Sec. IX (a) and with the method of Sec. XI (b). The number of walkers for each lattice size and figure (a) is $M = 1000, 2000, 3000, 3000, 3000$ with $k_p = 30, 50, 60, 80, 80$ and $l = 6, 8, 10, 12, 16$, respectively, while the guiding wave function is given by Eq. (21) with $\gamma = 1.125$. In (b) the number of walkers is $M = 1000, 2000, 2000, 2000$ and $k_p = 10, 20, 20, 25$.

verged values for m_l within the error bars even for the largest system size $N_a = 16 \times 16$. Note also that the “straight”-forward method converges much more quickly as the total spin is conserved in this method and the convergence to the ground state is determined by the much larger gap in the same singlet subspace. Our data for m_l are again in perfect agreement with Sandvik’s, who was able to obtain much smaller error bars. With the available data we have extrapolated m_l by displaying the ratio of this quantity with the spin-wave prediction in Fig. 4. The suppression of the finite-

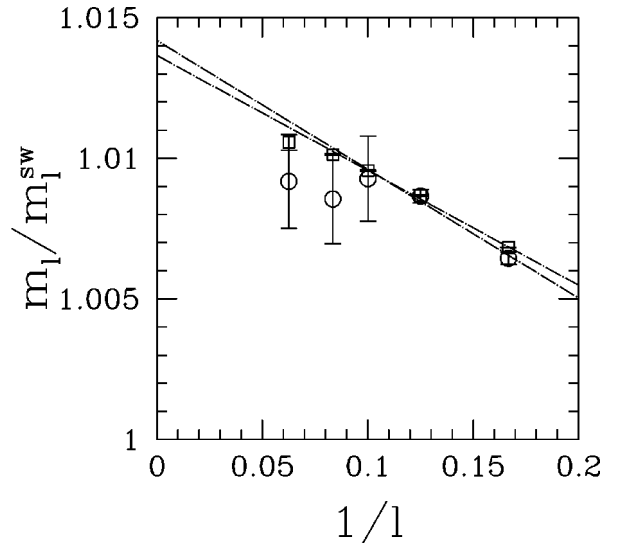


FIG. 4. Plot of the ratio between staggered magnetization, computed by the forward walking GFMC technique, and the spin-wave staggered magnetization as a function of $1/l$. The circles refer to the “straight”-forward walking technique (Sec. XI) and the squares to the data reported in Ref. 14. The lines are a weighted linear least squares fit of the data. The extrapolations for $l \rightarrow \infty$ are displayed in Tables II and III.

size effects, obtained with this analysis, is remarkably good (see Table II).

Finally we have computed the structure factor with the forward walking technique (Sec. IX) for several momenta. Analogously to the previous case for the order parameter, we have studied the ratio of the quantum Monte Carlo (QMC) data with the spin-wave prediction given by Eq. (39). This calculation shows that the spin-wave expression (39) is particularly accurate close to $q \sim Q$ but there is some deviation for small momenta. From Eq. (39) the small- q limit of the structure factor can be computed analytically in a spin-wave expansion: $S(q) = |q|/2\sqrt{2}(s - c') = 0.1073|q|$. The ratio between our QMC data and the second-order spin-wave prediction is shown in Fig. 5 and for small q it approaches the value 1.045 ± 0.01 , rather independently of the system size. This yields, by Eq. (32), a direct determination of the product

TABLE II. Staggered magnetization of the HM in the square lattice $l \times l$ with side l computed with the forward walking technique. The numbers in parentheses represent error bars in the last digits. The extrapolated values of our GFMC data for $N_a \rightarrow \infty$ are obtained by the fit shown in Fig. 4.

l	m_l^a	m_l^b	m_l^c	m_l^d
6	0.4581(2)	0.458074(3)	0.4583(3)	0.4579(1)
8	0.420(1)	0.421709(9)	0.4212(6)	0.4217(1)
10	0.397(3)	0.399214(9)	0.3988(8)	0.3991(6)
12	0.378(14)	0.38400(1)	0.380(2)	0.3834(6)
16	=	0.3647(1)	0.361(9)	0.3642(6)
∞	0.3075(25)	0.3070(3)	0.3058(12)	0.3077(4)

^aReference 8.

^bReference 14.

^cThis work, Sec. IX.

^dThis work, Sec. XI.

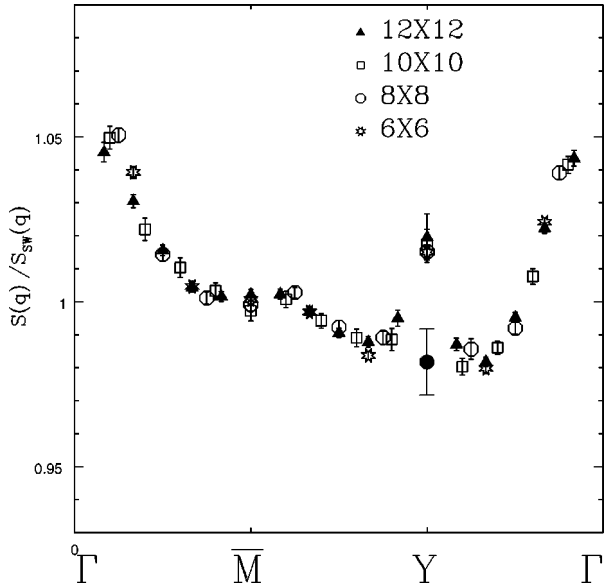


FIG. 5. Plot of the ratio between the spin-spin structure factor $S(q)$, computed by the forward walking GFMC technique, and the second-order spin-wave estimate $S_{SW}(q)$ [see Eq. (40)]. The structure factor has been evaluated for $L=6,8,10,12$ over the path $\Gamma = (0,0) \rightarrow \bar{M} = (\pi,0) \rightarrow Y = (\pi,\pi) \rightarrow \Gamma = (0,0)$. The large circle at the Y point is the expected $q \rightarrow Y$ limit of $S(q)/S_{SW}(q)$, by using the values for m^2 and χ_c reported in Table III.

of the spin-wave velocity and the susceptibility: $\chi_c = 0.1122 \pm 0.001$. This value is very much in disagreement with Sandvik's¹⁴ who predicted $\chi_c = 0.1046 \pm 0.002$, about four error bars out from our direct and more accurate result. This discrepancy is probably due to a very difficult infinite-size extrapolation of χ (Ref. 16) and c , whereas the product χ_c calculated by means of $S(q)$ for small momenta seems rather well behaved, as shown in Fig. 5. In the same figure the prefactor around $q \sim Q$ is in quite reasonable agreement with the expected one (large solid circle) m^2/χ_c obtained with our independent measures of χ_c (slope S_q for $q \rightarrow 0$) and $m^2[S(q)/N_a]$ for $q = Q$, considering also that this function, according to the Neuberger-Ziman theory, should jump discontinuously at $q = Q$, where it assumes a value determined only by the order parameter m^2 . The shape of the curve displayed in Fig. 5 is clearly consistent with the predicted singularity.

Our results therefore represent a direct confirmation of the internal consistency of the Neuberger-Ziman theory.

The values for the physical quantities extrapolated in the thermodynamic limit are summarized in Table III.

TABLE III. Infinite-size estimates of the various ground state quantities of the HM discussed in the paper. The value of m is obtained by fitting the more accurate data of Ref. 14 as shown in Fig. 4. The value of χ_c is computed from the data of Fig. 5, corresponding to the largest size and smallest momentum.

e_0	-0.669442(26)
m	0.3075 ± 0.0002
χ_c	0.1122 ± 0.001

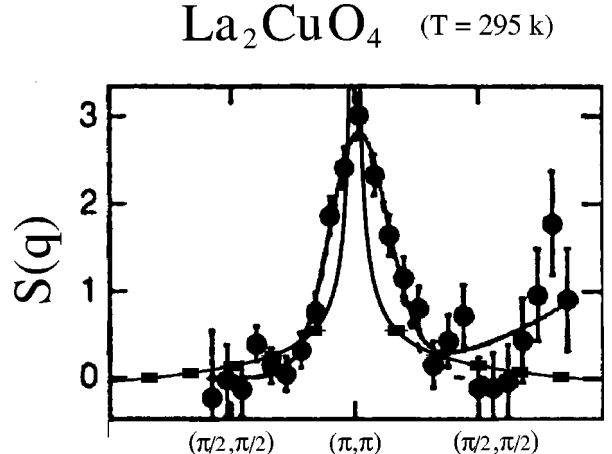


FIG. 6. Comparison between QMC data (solid squares) and experimental data (solid circles) for the static magnetic structure factor. The solid line connecting the QMC data is the second-order spin-wave prediction [see Eq. (40)], almost exact in this scale, whereas the line connecting the experimental data represents the corresponding fit reported in Ref. 5.

XIII. CONCLUSIONS

We have described in detail a straightforward implementation of the Green function Monte Carlo scheme on a lattice Hamiltonian without the need of the standard branching process. The extension of such a scheme to continuum systems such as ${}^4\text{He}$ is straightforward. Indeed the present algorithm works at a fixed number of walkers and we have shown that all sources of systematic error can be controlled with a rigorous approach both for computing the ground state energy and for computing ground state correlation functions. The possibility to work with a limited number of walkers is extremely important for high-accuracy calculations. This in fact requires quite long simulations to decrease the statistical errors and, with the standard approach,² one easily exceeds the maximum number of walkers for the available computer memory.

Our reconfiguration scheme is not restricted to work at a fixed number of walkers. In fact our proofs in Secs. VI and X can be readily generalized when the number M' of outgoing walkers x'_j (with unit weight) is different from the number M of the incoming ones w_j , x_j . Thus a standard branching scheme between two consecutive reconfigurations can be also applied, and the method can be used only each time the population of walkers reaches an exceedingly large or small size. At each stochastic reconfiguration the simple factor $\sum_{j=1}^M w_j/M'$ corrects exactly the bias of the described size population control. This maybe a more efficient implementation of our method, with, however, a rather more involved algorithm.

This scheme represents a more practical implementation of the Hetherington idea to work at fixed number of walkers as (i) it is not required to apply the reconfiguration process at each Markov iteration. Indeed our scheme coincides with the Hetherington one in this limit. (ii) The same idea to control the bias at fixed number of walkers was extended to the “forward walking technique” which is important to calculate efficiently correlation functions on the ground state. (iii) Contrary to the conventional belief we have shown that there

are no basic difficulties to compute “off diagonal” correlation functions with the Green function Monte Carlo technique, using a simple forward walking technique (Sec. XI), which turned out to be very efficient for determining the order parameter in the HM.

We have applied these methods to compute very accurately the ground state energy per site of the HM, the spin-spin structure factor, and the antiferromagnetic order parameter, whose infinite-size values are shown in Table III.

We have obtained very good agreement with finite-size spin-wave theory, which allows a very well-controlled finite-size scaling (see Fig. 5). We believe that the reported accuracy gives a very robust confirmation of the existence of antiferromagnetic (AF) long-range order in the 2D HM.

We finally show in Fig. 6 a comparison of our QMC prediction for $S(q)$ with the available experimental data on the stoichiometric La_2CuO_4 Mott insulator for momenta close to the AF wave vector: $q \sim (\pi, \pi)$. The agreement is remarkably good considering also that (i) the experiments have been performed at a temperature above the Néel temperature, so that no true long-range order exists, despite the very long correlation length.⁵ As a consequence, for a good comparison between experiments and theory, one should take into account the smearing of the δ function contribution at $Q = (\pi, \pi)$, to be added to the theoretical ground state prediction. (ii) There are no fitting parameters in the present comparison.

Therefore the copper-oxygen planes of La_2CuO_4 , planes which become high-temperature superconductors upon finite hole doping, are well described by the nearest-neighbor Heisenberg model.

ACKNOWLEDGMENTS

It is a pleasure to acknowledge useful discussions with C. Lavalle, L. Guidoni, and E. Tosatti. One of us (S.S.) wishes to thank the Institute for Nuclear Physics of Seattle for warm hospitality. This work is partly supported by PRA HTSC of the Istituto Nazionale di Fisica della Materia (S.S.).

APPENDIX: PRACTICAL RECONFIGURATION PROCESS

In this appendix we follow the notation of Sec. VI to describe an efficient implementation of the reconfiguration process needed to stabilize the proposed GFMC method.

The new walkers x'_i after reconfiguration are chosen among the old ones x_k , with probability p_k . We divide the interval $(0,1)$ in M subintervals with length p_k from the leftmost to the rightmost as k increases from 1 to M . Then we generate M pseudorandom numbers z_i for $i=1, \dots, M$ and sort them, bearing in mind that the index i labels the walker x'_i after the reconfiguration. We save therefore the random permutation $i(k)$, $k=1, \dots, M$, corresponding to the described sorting, the permutation that determines $z_{i(k+1)} > z_{i(k)}$. An efficient sorting algorithm takes the order of $M \ln M$ operations, and thus is not time consuming.

The next step is to make a loop over the sorted index k , giving a monotonically increasing $z_{i(k)}$, and to select as a new configuration $x'_{i(k)}$ the one x_j , among the old configurations, such that $z_{i(k)}$ belongs to the interval of length p_j . Note that the index function $j(i)$, $i=1, \dots, M$, contains all the information required for the forward walking technique described in Sec. IX.

After the described process some of the old configurations may appear in many copies, while others disappear. This happens also if the distribution p_j is uniform $p_j \sim 1/M$, yielding clearly some loss of information in the statistical process. A better way to implement the reconfiguration, without losing information and without introducing any source of systematic error, is obtained by the following simple change. After the generation of the random permutation $i(k)$ a new set of numbers uniformly distributed in the interval $(0,1)$ is defined:

$$\bar{z}_i = [\xi + (i-1)]/M$$

for $i=1, \dots, M$, where ξ is another pseudorandom number in $(0,1)$. This set of numbers \bar{z}_i , now uniformly distributed in the interval $(0,1)$, is then used to select the new configurations, yielding a more efficient implementation of the described reconfiguration process.

¹J. D. Reger and A. P. Young, Phys. Rev. B **37**, 5978 (1988).

²See, e.g., N. Trivedi and D. M. Ceperley, Phys. Rev. B **41**, 4552 (1990).

³P. W. Anderson, Phys. Rev. B **86**, 694 (1952).

⁴H. Neuberger and T. Ziman, Phys. Rev. B **39**, 2608 (1989).

⁵S. M. Hayden, G. Aeppli, M. A. Mook, T. G. Perring, T. E. Mason, S.-W. Cheong, and Z. Fisk, Phys. Rev. Lett. **76**, 1344 (1996).

⁶For a review and recent references, see, e.g., W. von der Linden, Phys. Rep. **220**, 53 (1992); H. De Raedt and W. von der Linden, in *The Monte Carlo Method in Condensed Matter Physics*, edited by K. Binder (Springer-Verlag, Heidelberg, 1992).

⁷D. M. Ceperley and M. H. Kalos, in *Monte Carlo Method in Statistical Physics*, edited by K. Binder (Springer-Verlag, Heidelberg, 1992).

⁸K. J. Runge, Phys. Rev. B **45**, 7229 (1992); **45**, 12 292 (1992).

⁹H. J. M. van Bemmelen, D. F. B. ten Haaf, W. van Saarloos, J. M. J. van Leeuwen, and G. An, Phys. Rev. Lett. **72**, 2442 (1994).

¹⁰D. F. B. ten Haaf, H. J. M. van Bemmelen, J. M. J. van Leeuwen, W. van Saarloos, and D. M. Ceperley, Phys. Rev. B **51**, 13 039 (1995).

¹¹J. H. Hetherington, Phys. Rev. A **30**, 2713 (1984).

¹²F. Franjic and S. Sorella, Prog. Theor. Phys. **97**, 399 (1997).

¹³D. Fisher, Phys. Rev. B **39**, 11 783 (1989).

¹⁴A. W. Sandvik, Phys. Rev. B **56**, 11 678 (1997).

¹⁵Q. F. Zhong and S. Sorella, Europhys. Lett. **21**, 629 (1993).

¹⁶C. Lavalle, S. Sorella, and A. Parola, Phys. Rev. Lett. **80**, 1746 (1998).